Shell Structure of the Near-Dripline Nucleus 23O

Shell Structure of the Near-Dripline Nucleus ^{23}O

D. Cortina-Gil,[1,2] J. Fernandez-Vazquez,[1] T. Aumann,[2] T. Baumann,[3] J. Benlliure,[1] M. J. G. Borge,[4] L. V. Chulkov,[2,5] U. Datta Pramanik,[2] C. Forssén,[6] L. M. Fraile,[4] H. Geissel,[2] J. Gerl,[2] F. Hammache,[2] K. Itahashi,[7] R. Janik,[8] B. Jonson,[6] S. Mandal,[2] K. Markenroth,[6] M. Meister,[6] M. Mocko,[8] G. Münzenberg,[2] T. Ohtsubo,[2] A. Ozawa,[9] Y. Prezado,[4] V. Pribora,[2,5] K. Riisager,[10] H. Scheit,[11] R. Schneider,[12] G. Schrieder,[13] H. Simon,[13] B. Sitar,[8] A. Stolz,[12] P. Strmen,[8] K. Sümmerer,[2] I. Szarka,[8] and H. Weick[2]

[1]*Universidad de Santiago de Compostela, E-15706 Santiago de Compostela, Spain*
[2]*Gesellschaft für Schwerionenforschung (GSI), D-64291 Darmstadt, Germany*
[3]*NSCL, Michigan State University, East Lansing, Michigan 48824, USA*
[4]*Instituto de Estructura de la Materia, CSIC, E-28006 Madrid, Spain*
[5]*Kurchatov Institute, RU-123182 Moscow, Russia*
[6]*Experimentell Fysik, Chalmers Tekniska Högskola och Göteborgs Universitet, SE-412 96 Göteborg, Sweden*
[7]*Department of Physics, University of Tokyo, 7-3-1 Hongo, Bunkyo-ku, Tokyo 113, Japan*
[8]*Faculty of Mathematics and Physics, Comenius University, 84215 Bratislava, Slovakia*
[9]*RIKEN, 2-1 Hirosawa Wako, Saitama 3051-01, Japan*
[10]*Institut for Fysik og Astronomi, Aarhus Universitet, DK-8000 Aarhus C, Denmark*
[11]*Max-Planck Institut für Kernphysik, D-69117 Heidelberg, Germany*
[12]*Physik-Deptartment E12, Technische Universität, München, D-85748 Garching, Germany*
[13]*Institut für Kernphysik, Technische Universität, D-64289 Darmstadt, Germany*

(Received 15 December 2003; published 6 August 2004)

Breakup reactions were used to study the ground-state configuration of the neutron-rich isotope ^{23}O. The ^{22}O fragments produced in one-nucleon removal from ^{23}O at 938 MeV/nucleon in a carbon target were detected in coincidence with deexciting γ rays. The widths of the longitudinal momentum distributions of the ^{22}O fragments and the one-neutron removal cross sections were interpreted in the framework of a simple theoretical model which favors the assignment of $I^\pi = 1/2^+$ to the ^{23}O ground state.

DOI: 10.1103/PhysRevLett.93.062501 PACS numbers: 25.60.Gc, 21.10.Pc, 25.60.Dz, 27.30.+t

For decades the nuclear shell model has been one of the most important tools to interpret a wealth of experimental data. With the advent of radioactive-beam facilities, the evolution of nuclear shell structure far from the valley of β stability could be studied. At present, such studies can be extended to the limits of bound nuclei on the neutron-rich side (the neutron dripline) for nuclear charges up to $Z = 8$, oxygen. An important tool in this context are high-energy knockout reactions of single neutrons from near-dripline nuclei. Brown *et al.* [1] have shown that the residue momentum distributions and the corresponding cross sections can be analyzed in such a way that both the l values and the single-particle occupation probabilities of the levels can be deduced. This, however, requires that the level from which the breakup occurred is identified uniquely by measuring γ rays in coincidence with the residue [2,3].

An interesting case to study is the series of neutron-rich oxygen isotopes near the neutron dripline. It has been shown recently that ^{22}O with a first excited 2^+ level at 3.17 MeV [4] and ^{24}O with no excited state below 4 MeV [5] seem to be doubly magic nuclei. This indicates a persistence of the proton-magic shell at $Z = 8$ and (sub) shell closures at $N = 14$ and $N = 16$. At the same time, the nonobservation of ^{28}O with 20 neutrons is indicative of a weakening of the $N = 20$ shell; the last bound oxygen isotope is ^{24}O [6–9]. The tentative assignment of ^{24}O having a closed $(s_{1/2})^2$ shell was corroborated by Sauvan *et al.* [10,11] who measured a relatively narrow longitudinal momentum distribution of ^{22}O after one-neutron knockout from ^{23}O, leading to a ground-state spin and parity of $I^\pi = 1/2^+$ for ^{23}O. In contrast, Kanungo *et al.* [12] attributed $I^\pi = 5/2^+$ to the ^{23}O ground state. If confirmed, this would have significant ramifications for our understanding of the shell structure in the vicinity of $N = 16$. This controversy prompted a comment by Brown *et al.* [13] and calculations by Sauvan *et al.* [11]. Both papers give a consistent analysis of the available *inclusive* data in terms of a $(d_{5/2})^6(s_{1/2})^1$ configuration for ^{23}O.

As mentioned above, the experimental confirmation of such a theoretical analysis requires an *exclusive* knockout experiment where the individual levels are identified by measuring in coincidence the deexciting γ rays. We have performed such an exclusive experiment at the fragment separator FRS at Gesellschaft für Schwerionenforschung (GSI) in Darmstadt, Germany. The primary beam was ^{40}Ar at 1 GeV/nucleon delivered by the SIS synchrotron with an average intensity of 1.5×10^{10} particles/spill. The secondary ^{23}O fragments were produced by nuclear

fragmentation of the primary beam in a Be target located at the entrance of the FRS. A detailed description of the experimental setup has been presented in Refs. [14,15]. The first half of the FRS was set to transport the secondary ^{23}O beam (938 MeV/nucleon) to the intermediate focal plane, where the breakup on a C target took place. The average rate of ^{23}O projectiles on the target amounted to six ions per second. Complete identification of the secondary beams was achieved by measuring the time of flight between two plastic detectors and by energy-deposition measurements in an ionization chamber. The second half of the spectrometer was set to the magnetic rigidity of the emerging ^{22}O breakup fragments. The identification of those fragments was performed in a similar way as for the secondary projectiles. This unambiguous double identification ensures a clean reaction channel selection.

The fragment longitudinal momentum distributions were measured by using time projection chambers. Coincident γ rays were detected in an array of 32 NaI detectors (hexagons 3.5 cm side) placed 80 cm downstream of the breakup target. The detectors were mounted in four rectangular frames surrounding the central spectrometer axis providing 20×15 cm^2 free space for transmission of the fragments. Each detector subtended a different angle relative to the breakup point. This array has an average energy resolution ($\Delta E/E$) of $(12.0 \pm 0.8)\%$ and a total efficiency of $(5.0 \pm 0.4)\%$ for the case of γ rays emitted by relativistic moving sources (obtained from a GEANT [16] simulation for $E_\gamma = 3.2$ MeV in the rest frame of the fragment). The FRS was operated in its energy loss mode [17] using a special ion optic that ensures the measurement of the complete momentum distribution in one single setting. The intrinsic momentum resolution for ^{23}O was evaluated to be 19 ± 1 MeV/c (FWHM). This experimental value includes the ion optical properties of the FRS plus straggling in the target, optical misalignment, and any other secondary effects.

The inclusive one-neutron removal cross section (σ_{-1n}) of ^{23}O was measured by directly counting ^{23}O and ^{22}O in front of and behind the carbon breakup target. This ratio was corrected for the experimental transmission evaluated with the code MOCADI [18] after adjusting the simulated fragment longitudinal momentum width to the measured one. The value obtained was $\sigma_{-1n} = 85 \pm 10$ mb. The error includes statistical and transmission errors. We present this result in Table I together with the σ_{-1n} evaluated for other neutron-rich nuclei in this experiment [19].

The cross section is larger than the ones measured at relativistic energies for stable isotopes (e.g., σ_{-1n} for ^{12}C at 1050 MeV/nucleon on a C target amounts to 44.7 ± 2.8 mb [20]) but follows a systematic increasing trend with mass number A (see Table I). The result can be compared with the one from an experiment performed at 72 MeV/nucleon [12] that gave $\sigma_{-1n} = 233 \pm 37$ mb. In contrast to the situation found for p_{long}, which will be discussed below, the difference in primary beam energy has a strong influence on the final σ_{-1n} and a proper comparison between these results has to be performed with the help of theoretical models. The differential cross section with respect to longitudinal momentum p_{long} (in the projectile center-of-mass frame) is shown on the left panel of Fig. 1 for the one-neutron removal reaction. The solid curve corresponds to a double Gaussian fit to the experimental data from which a width of 134 ± 10 MeV/c (FWHM) was obtained. A minor correction for the intrinsic momentum resolution gives a final width of 133 ± 10 MeV/c. This result can be directly compared to the corresponding value of 114 ± 9 MeV/c (FWHM) obtained at 47 MeV/nucleon [10] and of 73 ± 15 MeV/c

TABLE I. Summary of results from inclusive measurements for different neutron-rich oxygen isotopes. The second column lists the average energy of the secondary projectiles, the one-neutron removal cross section is shown in the third column, and the fourth column contains the width (FWHM) of the corresponding longitudinal momentum distributions of the fragments after one-neutron removal in the rest frame of the projectile.

Projectile	E MeV/nucleon	σ_{-1n} mb	FWHM MeV/c
^{19}O	935	56 ± 7	183 ± 10
^{20}O	936	56 ± 6	199 ± 10
^{21}O	937	72 ± 7	190 ± 10
^{22}O	937	70 ± 7	206 ± 10
^{23}O	938	85 ± 10	133 ± 10

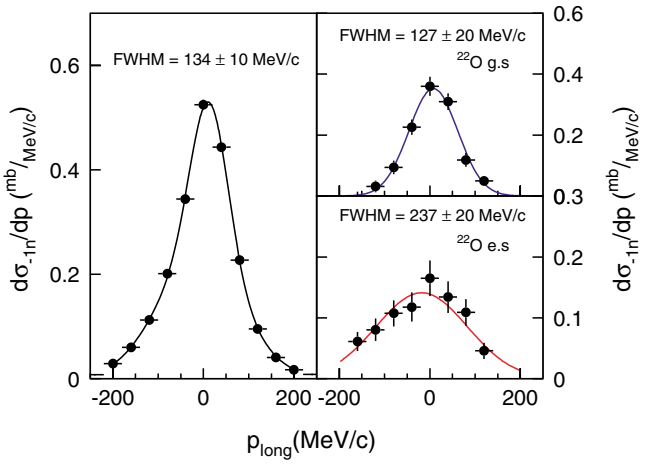

FIG. 1 (color online). Left: Inclusive longitudinal momentum distribution (p_{long}) for ^{22}O fragments after one-neutron removal from ^{23}O. Right, top: Exclusive longitudinal momentum distribution for ^{22}O in its ground state. Right, bottom: Longitudinal momentum distribution for ^{22}O in any excited state.

at 72 MeV/nucleon [12]. In Table I the FWHM of the longitudinal momentum distribution evaluated for other neutron-rich oxygen isotopes in this experiment [19] is presented. As can be seen from this compilation, a rather constant width is observed for the neutron-rich oxygen isotopes up to $A = 22$, followed by a significant reduction for ^{23}O, which indicates the crossing of the $N = 14$ subshell closure and the occupation of the $2s_{1/2}$ orbital.

The γ rays emitted during deexcitation of ^{22}O were recorded with the NaI detectors described above. The high-energy γ rays and the emission of γ rays in cascade make it necessary to apply addback corrections. Subsequently, we performed a Doppler shift correction. We applied an extra filter on the final reconstructed good events (those obtained after the corrections mentioned above), selecting multiplicity equal one exclusively. This filter allows one to improve considerably the peak-to-background ratio on the final γ ray spectrum that is presented in Fig. 2. The limited granularity of the setup causes a substantial Doppler broadening being the dominant contribution to the obtained resolution. The points in Fig. 2 representing the experimental measurement are compared with a solid line that is obtained from the complete GEANT simulation of our experiment including an exponential background [14,15,19].

The analysis of the γ ray spectrum reveals three γ ray energies at 1.3, 2.6, and 3.2 MeV corresponding to the known transitions in ^{22}O [4,5,13] (see the level scheme in Fig. 2.) They correspond to deexcitation of the 2^+ and 3^+ states at 3.2 and 4.5 MeV, respectively, resulting from a $1d_{5/2}$ hole coupled to a $2s_{1/2}$ particle. The 5.8 MeV state could be due to the 0^- or/and 1^- states proposed in [13].

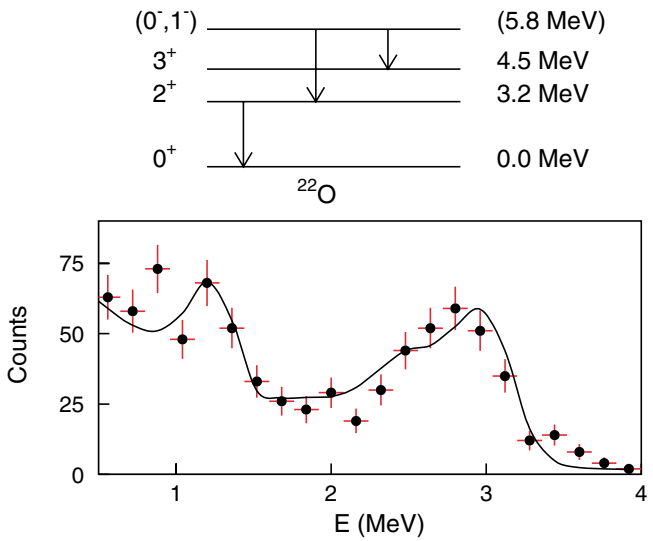

FIG. 2 (color online). Spectrum of γ rays in coincidence with ^{22}O fragments after one-neutron removal from ^{23}O in a carbon target. The spectrum shown has been obtained from the measured γ-ray spectrum (see text). The experimental spectrum is compared with the result of a GEANT simulation adopting the level scheme shown above.

The broad peak observed at higher energy is assumed to be due to the 3.2 MeV and the 2.6 MeV transitions that our NaI detectors cannot resolve. The inclusion of the cascade from the 5.8 MeV state yields a significantly improved description of the experimental spectrum by the simulation. We assume that all the ^{22}O excited levels decay through the first excited state at 3.2 MeV. This peak is, therefore, used to gate the longitudinal momentum distribution in order to obtain the exclusive distribution. The result, after efficiency correction of the γ array evaluated with a GEANT simulation and proper background subtraction, is shown in the right, bottom panel of Fig. 1, where the solid line corresponds to the Gaussian fit performed to obtain the width of the distribution. This results in a FWHM of 236 ± 20 MeV/c for the momentum distribution leaving the core in any excited state.

The longitudinal momentum distribution for ^{22}O in its ground state could be obtained by subtracting from the inclusive measurement the exclusive one involving ^{22}O in any of its excited states. The resulting spectrum is shown in the right, top panel of Fig. 1. We obtain a FWHM of 126 ± 20 MeV/c (after correcting for the intrinsic momentum resolution). The corresponding integrated cross section amounts to 50 ± 10 mb. A summary of the experimental results obtained for ^{23}O is given in Table II (third and fourth columns). The associated error bars include statistical errors, assumptions for the level scheme of ^{22}O, and uncertainties in the γ-efficiency simulation. The relative weight of the exclusive one-neutron removal cross section involving ^{22}O in any excited states to the inclusive measurement amounts to (41 ± 10)%.

The experimental momentum distribution for the one-neutron removal-channel leaving the ^{22}O core in its ground state is compared in Fig. 3 to theoretical momentum distributions calculated in an eikonal model for the knockout process. [21].

Two calculations are shown for angular momenta $l = 0$ and $l = 2$. Clearly, the distribution assuming a $2s_{1/2}$

TABLE II. Experimental widths (FWHM) of longitudinal momentum distributions in the projectile rest frame (third column) The experimental one-neutron removal cross sections (fourth column) and spectroscopic factors (sixth column) are presented for $^{23}\mathrm{O} \rightarrow {}^{22}\mathrm{O} + n$ in the different final state configurations considered. Calculated cross sections and spectroscopic factors shown in the fifth and seventh columns, respectively, for comparison.

E MeV	I^π	FWHM MeV/c	σ_{exp} mb	σ_{sp} mb	S_{exp}	C^2S [13]
0	0^+	126 ± 20	50 ± 10	51	0.97 ± 0.19	0.80
3.2	2^+	236 ± 20	10.5 ± 4.5	20	0.52 ± 0.21	2.13
4.5	3^+		14.0 ± 5.0	18	0.77 ± 0.27	3.08
5.8	$(1^-, 0^-)$		10.5 ± 4.5	15	0.70 ± 0.28	0.85(0.33)
Total		133 ± 10	85 ± 10	104		

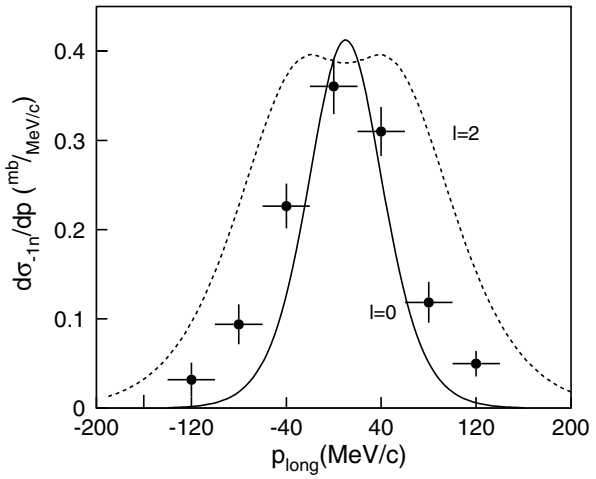

FIG. 3. Ground-state exclusive momentum distribution for ^{22}O fragments after one-neutron knockout reaction from ^{23}O compared with calculations assuming $l = 0$ and $l = 2$ (see text).

neutron coupled to the $^{22}O(0^+)$ core is in much better agreement with the data. We can thus conclude that the ground-state spin of ^{23}O is $I^\pi = 1/2^+$. We note, however, that the experimental distribution is slightly wider than the prediction for $l = 0$. This might be due to a slightly incomplete subtraction of the excited-state contribution. The large width of 237 ± 20 MeV/c observed for the distribution involving excited states is in line with the expectation that, in this case, most of the cross section is related to the knockout of neutrons from the d shell.

We now turn to the one-neutron removal cross sections, which are calculated separately for the individual single-particle configurations adopting the eikonal approach [22,23], which is well justified at the high beam energy used in the present experiment. The neutron-core relative-motion wave functions are calculated for a Woods-Saxon potential with geometry parameters of $r_0 = 1.25$ fm and $a = 0.7$ fm [2,3]. Further input to the calculations are free nucleon-nucleon cross sections and harmonic-oscillator density distributions for the target and the core, which were chosen to reproduce the measured interaction cross sections at high energy [24].

Neutron-knockout cross sections were calculated for the configuration $(d_{5/6})^6$ $(s_{1/2})^1$ and are summarized in the fifth column of Table II. For the neutron knockout from the $2s$ shell, the calculated cross section is equal to 51 mb and thus is in agreement with the experimental value of 50 ± 10 mb. This result confirms the large spectroscopic factor for the s-neutron ($C^2S = 0.8$) obtained by Brown *et al.* [13] . The knockout of a neutron from the $1d$ shell in this calculation results in ^{22}O either in the 2^+ state (20.0 mb) or in the 3^+ state (18.3 mb). The contribution of the knockout of neutrons from deeper p shells ($1^-, 0^-$ state) amounts to 15 mb. A comparison with the experimental data shows that the contribution involving excited states is smaller by a large factor. The discrepancy might to a large extent be related to the deficiencies of the simple single-particle model we used and points towards the need of more elaborate reaction models for calculating knockout cross sections from the deeply bound core states. A further investigation of this is certainly needed but goes beyond the scope of the present work.

In conclusion, we have measured the ^{22}O momentum distribution after one-neutron knockout from high-energy ^{23}O projectiles differentiated according to states populated in ^{22}O observed by a coincident measurement of the ^{22}O γ deexcitation. The experimental observations are evidence for a ground-state spin $I^\pi = 1/2^+$ for ^{23}O with a large spectroscopic factor for the $s_{1/2} \otimes {}^{22}O(0^+)$ single-particle configuration, thus providing support for the existence of the $N = 14$ and $N = 16$ subshell closures for $Z = 8$.

The authors are indebted to P. G. Hansen and B. A. Brown for valuable discussions. This work was supported by EU (ERBFMGECT95 0083), Internationales Büro Osteuropa-Verbindungsbüro des BMBF bei den DLR (WTZ Bonn SLA-002-96-BMBF and 06DA915I), NFR Sweden (F5102-1484/2001), and MCyT, Spain (FPA-2001-C05-4-01).

[1] B. A. Brown *et al.*, Phys. Rev. C **65**, 061601(R) (2000).
[2] T. Aumann *et al.*, Phys. Rev. Lett. **84**, 35 (2000).
[3] V. Maddalena *et al.*, Phys. Rev. C **63**, 024613 (2001).
[4] P. G. Thirolf *et al.*, Phys. Lett. B **485**, 16 (2000).
[5] M. Stanoiu *et al.*, Phys. Rev. C **69**, 034312 (2004).
[6] O. Tarasov *et al.*, Phys. Lett. B **409**, 64 (1997).
[7] A. Ozawa *et al.*, Nucl. Phys. **A673**, 411 (2000).
[8] H. Sakurai *et al.*, Phys. Lett. B **448**, 180 (1999).
[9] M. Thoennessen *et al.*, Phys. Rev. C **68**, 044318 (2003).
[10] E. Sauvan *et al.*, Phys. Lett. B **491**, 1 (2000).
[11] E. Sauvan *et al.*, Phys. Rev. C **69**, 044603 (2004).
[12] R. Kanungo *et al.*, Phys. Rev. Lett. **88**, 142502 (2002).
[13] B. A. Brown, P. G. Hansen, and J. A. Tostevin, Phys. Rev. Lett. **90**, 159201 (2003).
[14] D. Cortina-Gil *et al.*, Phys. Lett. B **529**, 36 (2002).
[15] D. Cortina-Gil *et al.*, Nucl. Phys. **A720**, 3 (2003).
[16] GEANT 3.2.1, CERN Library Report No. W5013, 1993.
[17] H. Geissel *et al.*, Nucl. Instrum. Methods Phys. Res., Sect. B **70**, 286 (1992).
[18] N. Iwasa *et al.*, Nucl. Instrum. Methods Phys. Res., Sect. B **126**, 284 (1997).
[19] J. Fernadez, Ph.D. thesis, Universidad de Santiago de Compostela, 2003.
[20] D. L. Olson *et al.*, Phys. Rev. C **28**, 1602 (1983).
[21] P. G. Hansen, Phys. Rev. Lett. **77**, 1016 (1996).
[22] J. Tostevin, J. Phys. G **25**, 735 (1999).
[23] G. F. Bertsch, K. Hencken, and H. Esbensen, Phys. Rev. C **57**, 1366 (1998).
[24] A. Ozawa *et al.*, Nucl. Phys. **A693**, 32 (2001).